Multiscale Aspects of Thunderstorm Gust Fronts and Their Effects on Subsequent Storm Development

JOHN F. WEAVER[1]

RAMM Branch/NOAA/NESS, Colorado State University, Ft. Collins 80523

STEPHAN P. NELSON

National Severe Storms Laboratory, Norman, OK 73069

(Manuscript received 28 May 1981, in final form 11 March 1982)

ABSTRACT

An investigation of severe storms that occurred on 23 May 1974 in central Oklahoma reveals interesting information on the multifaceted role of thunderstorm-produced gust fronts. The data reveal that the interaction of outflow boundaries with a cold front initiate the storms studied in this report. Then, the gust fronts produced by these storms have important effects on their own structure and life histories. Detailed Doppler analysis show that these storms propagate *discretely* along their outflow boundaries despite their supercell structure. Additionally, one storm is affected by its interaction with the boundary produced by a previous storm. This interaction appears responsible for tornadogenesis.

1. Introduction

Over the years, narratives describing thunderstorms have included accounts of intense, cool winds in advance of the onset of precipitation. The phenomenon, and its importance in the environment, were recognized early by meteorologists. For example, in his book *The Philosophy of Storms*, Espy (1841), states ". . . a violent summer shower often causes the wind to blow outward . . . from the shower. . . . The wind at some considerable distance from the falling shower, still continues to blow towards the rain, glancing up over the outmoving current. In this way, new columnar clouds are seen to form rapidly to the windward of the rain cloud."

With the 20th century came increasingly more precise understanding of the outflow phenomenon. McFarland (1901) suggested that the downrush of air in the storm (already understood to be the cause of the outflow) might result as much from the negative buoyancy of rain-cooled air as from frictional drag of falling particles (then generally thought to be the primary cause of downdrafts). As to the mechanism of rain cooling, he mentioned both conductive and evaporative effects. Utilizing case study data, Humphreys (1914) clarified the thermodynamics and kinematics of the downdraft, accepting the concept of rain-induced negative buoyancy, but relegating frictional drag to a minor, contributory role. Suckstorff (1939) analyzed case study data to verify a detailed downdraft model in which a major component was a small-scale anticyclone. He labeled this feature the "thunderstorm high." Harrison and Orendorff (1941) studied the pre-cold frontal wind shift line. Their report found the line to be a pseudo-cold-front on the leading edge of a mass of rain-cooled air. This pseudo-front seemed to contribute to the maintenance of thunderstorm squall lines. Tepper (1950) suggested that thunderstorms can be triggered by the passage of such "fronts" and Fujita (1960) subsequently verified this important characteristic.

Recent work on thunderstorm outflow includes kinematic and dynamic descriptions (Goff, 1976), case studies of thunderstorm growth and intensification via outflow (Holle and Meier, 1980), and detection methods such as the mesoscale analytical techniques suggested by Fujita (1958) and Barnes (1973) or satellite identification methods (Purdom, 1973). Other studies suggest that several types of interactions between storm outflow and other atmospheric features may occur quite frequently. Pseudo-cold-fronts alone may trigger activity (Fujita, 1960). Probabilities of storm initiation are markedly higher when and where outflow boundaries intersect other air mass boundaries (Purdom, 1976). In fact, recent data from the southeastern United States, collected during the summer of 1979, indicates 73% of all afternoon thunderstorms (~10 000 cases) form as a result of outflow interaction (Purdom and Marcus, 1982).

[1] Previous affiliation: National Severe Storms Laboratory, Norman, OK.

In the current study, data from a variety of sensors (including satellite, Doppler radars, surface stations and meteorologically trained observers) are utilized to investigate several thunderstorms that occurred in Kansas and Oklahoma on 23 May 1974. The data indicate that gust fronts produced by such storms are important on many scales and are factors in storm formation, propagation and intensification.

In the course of synthesizing the data for this case, a few interesting and unexpected facts emerged regarding storm structure. It was found, for example, that even though the storms exhibited classical supercell structure (Marwitz, 1972; Browning and Foote, 1976), they possessed multiple updrafts and propagated in a discrete manner.

2. Overview and synoptic conditions

a. Descriptive synopsis

An east–west line of thunderstorms developed in northern Oklahoma during the early afternoon of 23 May 1974. As the afternoon progressed the storms moved southeastward into the National Severe Storms Laboratory (NSSL) study area (see Fig. 1). At approximately 1640[2], a hook echo formed on the southern edge of a cell to the north of NSSL's Norman Doppler radar (NOR in Fig. 1) and was observed for about one hour. A strong, well-organized circulation was detected on Doppler throughout most of this period. The storm (named the Omega storm) produced 5 cm diameter hail and at least two funnel clouds before it moved out of the primary study area and died.

Meanwhile, a second large storm (called herein the Yukon storm) to the west of the Omega storm had intensified. It developed a hook echo on its southern edge and at 1740 data sensors were concentrated on it as it approached NSSL's Cimarron (CMF in Fig. 1) Doppler site 42 km northwest of NOR. Indications of a developing circulation on Doppler radar were coincident with reports of 4 cm diameter hail, strong low-level outflow winds and, finally, an F1 tornado (Fujita and Pearson, 1976) south of Yukon, Oklahoma.

b. Synoptic/subsynoptic description and storm initiation

Synthesis of 0600 synoptic data clearly suggested a severe thunderstorm potential for northern and central Oklahoma. A surface cold front had become stationary along the northern Oklahoma border and extended westward into New Mexico where a low had formed. A dry line was situated on a N–S orientation through western Texas near the Oklahoma border. Both 300 and 500 mb analyses indicated a minor short-wave trough west of Oklahoma, over western portions of New Mexico. Flow at 850 mb was southerly and moderately moist (although no advective moisture increase was indicated for Oklahoma).

A sounding, released from Fort Sill, Oklahoma at 1110, established that the air mass was potentially unstable. Allowing for an afternoon temperature of 85°F (as later occurred in central Oklahoma), the Lifted Index (Galway, 1956) was found to be −7. Winds aloft were moderately intense. Computed wind shear was 1.0×10^{-2} s^{-1} from the surface to 2 km AGL and 3×10^{-3} s^{-1} in the cloud bearing layer.

By midday a group of pre-existing thunderstorms in Kansas had pushed an outflow boundary into Oklahoma (Fig. 2) which began to bulge south-southwestward into north-central and northeastern portions of the state. Movie loops of visual satellite imagery clearly depict the advance of the arc-cloud throughout the afternoon (Fig. 3). Furthermore, the loops (see also Fig. 3) indicate that new convective activity was triggered at the intersection point of this arc-cloud with the synoptic-scale cold front. The southwestward propagation of this intersection point furnishes an explanation for an initial mystery; namely, the westward progression of new convective activity while the only other potential trigger (i.e., the short-wave trough aloft) was moving eastward. Additionally, the storms seemed to be associated with this boundary during the remainder of the afternoon.[3]

The outflow-induced cold front crossed the NSSL subsynoptic surface network during the late afternoon, traveling from 010° at 12.5 m s^{-1}. Storm motion (from 305° at 15 m s^{-1}) appeared to be a combination of the advective westerly flow aloft (mean cloud layer wind in a sounding taken at Norman, Oklahoma at 1717 was from 275° at 17.5 m s^{-1}), a southerly propagational component due to new updraft formation along each storm's own gust front, and convergence along the older thunderstorm boundary (Weaver, 1979).

3. Storm structures

A detailed investigation of the two primary storms on this day showed that gust fronts were important in ways other than providing enhanced convergence for storm initiation. These boundaries also appear to be directly related to storm structure, propagation

[2] All times Central Standard (CST).

[3] The strongest activity occurred along and near the outflow boundary rather than along the dryline as expected. Storms did form later along the weak dry frontal zone on 23 May, but they did not become as intense as the northern activity.

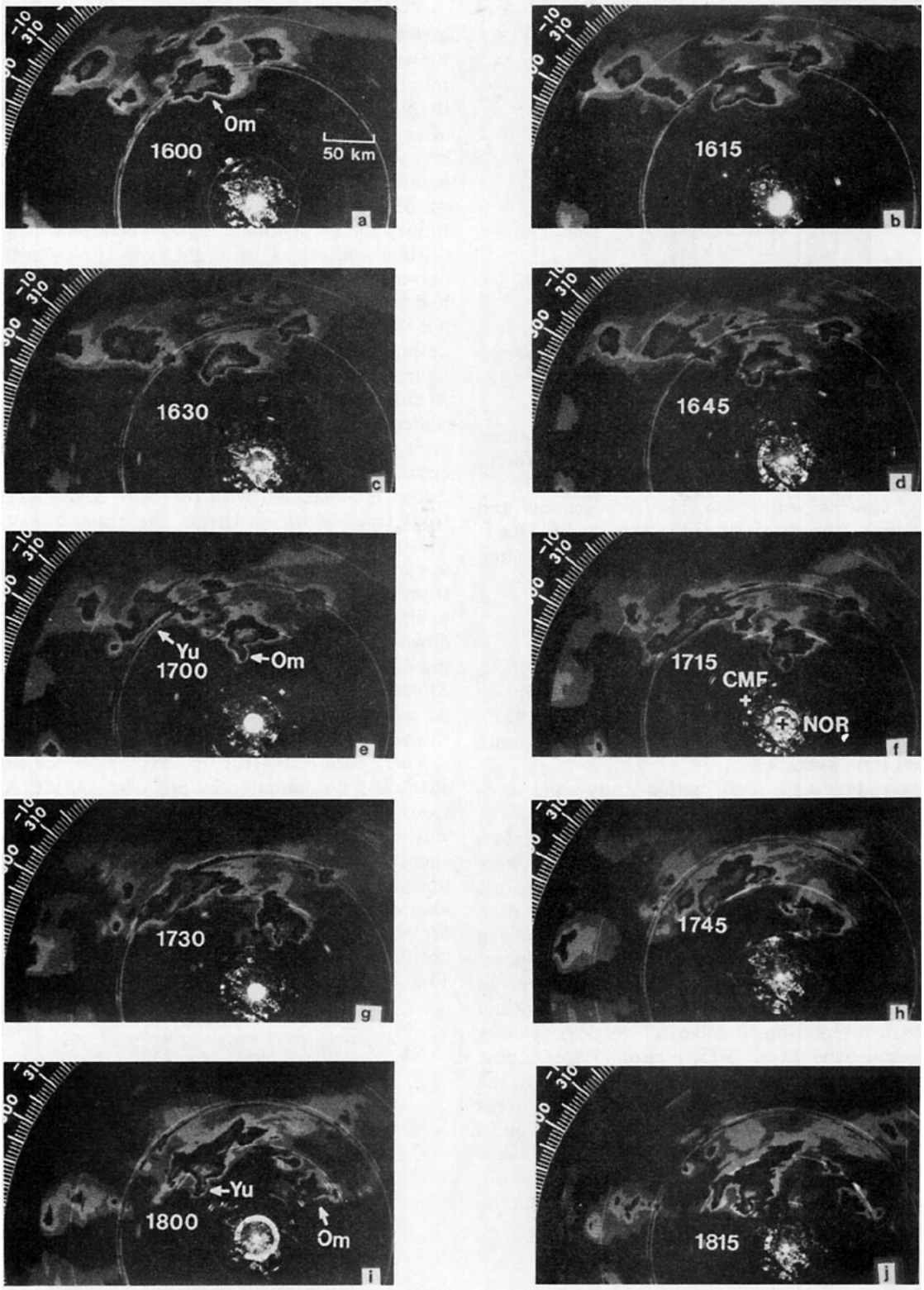

FIG. 1. NSSL WSR-57 radar reflectivity (0° tilt) at 15 min intervals from 1600 to 1815 CST. The Omega and Yukon storms are indicated by the "Om" and "Yu", respectively. Location of Norman (NOR) and Cimarron (CMF) Doppler radars are shown on the 1715 picture. Gray shade reflectivity calibrations: light gray–22 dB(Z); bright–33 dB(Z); dark–42 dB(Z); light gray–49 dB(Z); bright–57 dB(Z).

FIG. 2. ATS-3 satellite pictures at 1102 CST showing beginnings of outflow boundary (arrow) from storms in Kansas.

and intensification with the latter effect being caused by the interaction of gust fronts from different storms.

The following subsection describes sources and limitations of the data utilized in this study. This is followed by descriptions of the Omega and Yukon storms, and their interaction.

a. Data sources

Surface wind data were obtained from the NSSL subsynoptic and mesonetwork stations. A description of the instrumentation can be found in Staff (1971). Wind speed and direction were obtained from 5-min centered time averages.

Three radars were used in this study—the incoherent NSSL WSR-57 (Wilk and Kessler, 1970), and the coherent Norman and Cimarron radars (Alberty *et al.*, 1977). Dual Doppler wind fields were synthesized from the latter two radar measurements (e.g., Armijo, 1969; Brown *et al.*, 1981), but the data were somewhat limited due to insufficient signal in the storms' low-level notches and weak echo regions. In addition, the Cimarron Doppler did not scan to the storm top which forced use of upward rather than downward integration to solve for vertical velocity (Bohne and Srivastava, 1975, Nelson, 1980). These two factors combined to prevent solutions for the storm's weak echo regions. In addition, in areas where vertical velocities were obtained, no significance could be given to these values above the lowest few kilometers due to error amplification (Ray *et al.*, 1980). These errors, however, have little effect on the horizontal velocities.

b. Omega storm

Overall storm disposition is shown by the 0° tilt, PPI presentation of reflectivity[4] structure presented in Fig. 1. As the storm moved from the northwest it gradually strengthened with the reflectivity field showing a major structural change from several roughly east–west aligned "notches" in the reflectivity field to one very large north–south aligned hook after 1645. Detailed analysis of the reflectivity data revealed that these notches were associated with bounded weak echo regions (BWER) aloft (see Fig. 4). Many of these BWER's possessed temporal continuity and are assumed to be associated with several distinct updrafts. One might expect the storm to be dominated by only one updraft after the single hook had formed; however, the data indicate that this was not the case. That is, the multiple BWER's persisted despite the transition of the reflectivity field to a configuration more often associated with supercell storms. A dual-Doppler wind field synthesis at 1710 is presented in Fig. 5. The low-level data reveal features typically associated with a supercell storm. A strong circulation (maximum vorticity of 2.5×10^{-2} s^{-1} at 2 km) is associated with the hook echo and a gust front trails southward from the circulation center. The gust front demarcates the boundary between upper-level air transported to the surface and inflow from the southeast. This area of intense downdraft behind the gust front has been termed the rear flank downdraft. It is probably caused by evaporative cooling of entrained dry mid- or upper-level air and its existence is thought to be a common feature of supercell storms (Nelson, 1977; Burgess *et al.*, 1977; Barnes, 1978; Lemon and Doswell, 1979).

The updraft structure is fairly complex and the storm is not dominated by just one updraft. As previously noted, near 1615 the storm possessed several west-southwest to east-northeast aligned BWER's (hence, presumably several updrafts). The multiple updraft structure persists with time, but becomes aligned in a north–south direction. These features are shown in Fig. 6 which displays the horizontal position of the storm's major BWER's from 1615 to 1745.

FIG. 3. As in Fig. 2 except at 1446 CST showing progression of outflow boundary into Oklahoma.

[4] Reflectivity is used here to mean equivalent reflectivity factor.

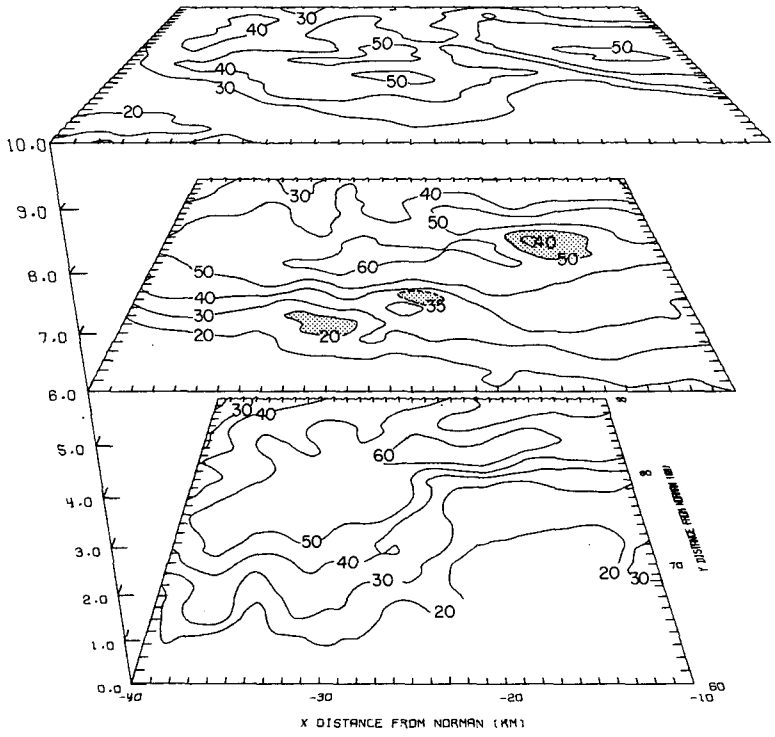

FIG. 4. Three-dimensional perspective view of Omega storm reflectivity field [dB(Z)] at 1640 CST. Bounded weak echo regions are indicated by the shaded areas. The vertical scale has been expanded by a factor of 2.

Details of three updrafts at 1710 can be seen in Figs. 5 and 7. The first updraft (labeled A on the 4 km section of Fig. 5) appears in the computed vertical velocity field and is nearly colocated with the circulation center. Even though there is an associated weakness in the low-level reflectivity field, there is no BWER aloft indicating that this updraft is beginning to decay (the reader is again reminded that the vertical velocity magnitudes are likely in error above the lowest few kilometers).

The remaining two updrafts are inferred from BWER's since a dual-Doppler synthesis is not possible here (see Section 3a). These updrafts are labeled B and C on the 10 km section of Fig. 5 and are shown in the vertical sections of Fig. 7. Further evidence for the existence of these updrafts was furnished by trained observers of the NSSL Tornado Intercept Project. At this time, their reports and photographs indicate rapid development of several flanking towers in this region. Particular note was made of the convective nature of the activity in the vicinity of the reported hook echo. The vertical section of updraft C reveals a fairly vertical reflectivity structure with a tight gradient; whereas, updraft B is sloped and not as well defined. This indicates updraft C is more vigorous and probably somewhat younger than B.

It certainly appears from the above data that this storm possessed several updrafts rather than the single updraft that is usually postulated for supercell storms (Marwitz, 1972; Browning and Foote, 1976). We hypothesize that as the rear flank downdraft becomes established, it forms an intense surface gust front that propagates southeastward and serves as the site for new updraft formation. That is, an updraft forms on the southwest end of the gust front and moves roughly with the environmental winds toward the east-southeast. As it matures, precipitation loading and/or other unidentified factors cause the updraft to decay as a new one forms further south along the gust front. The periodicity of updraft formation in this case is not known due to inadequate time-resolution of available data. It is believed that gust front formation and propagation causes the observed changes in updraft orientation. It would appear from Figs. 1 and 6 that the gust front slowly, but continually, advances in front of the storm eventually cutting off the inflow air and causing the storm's demise near 1745.

c. Yukon storm and storm interaction

The life history of the Yukon and Omega storms are very similar (see Fig. 1). Both storms emerged

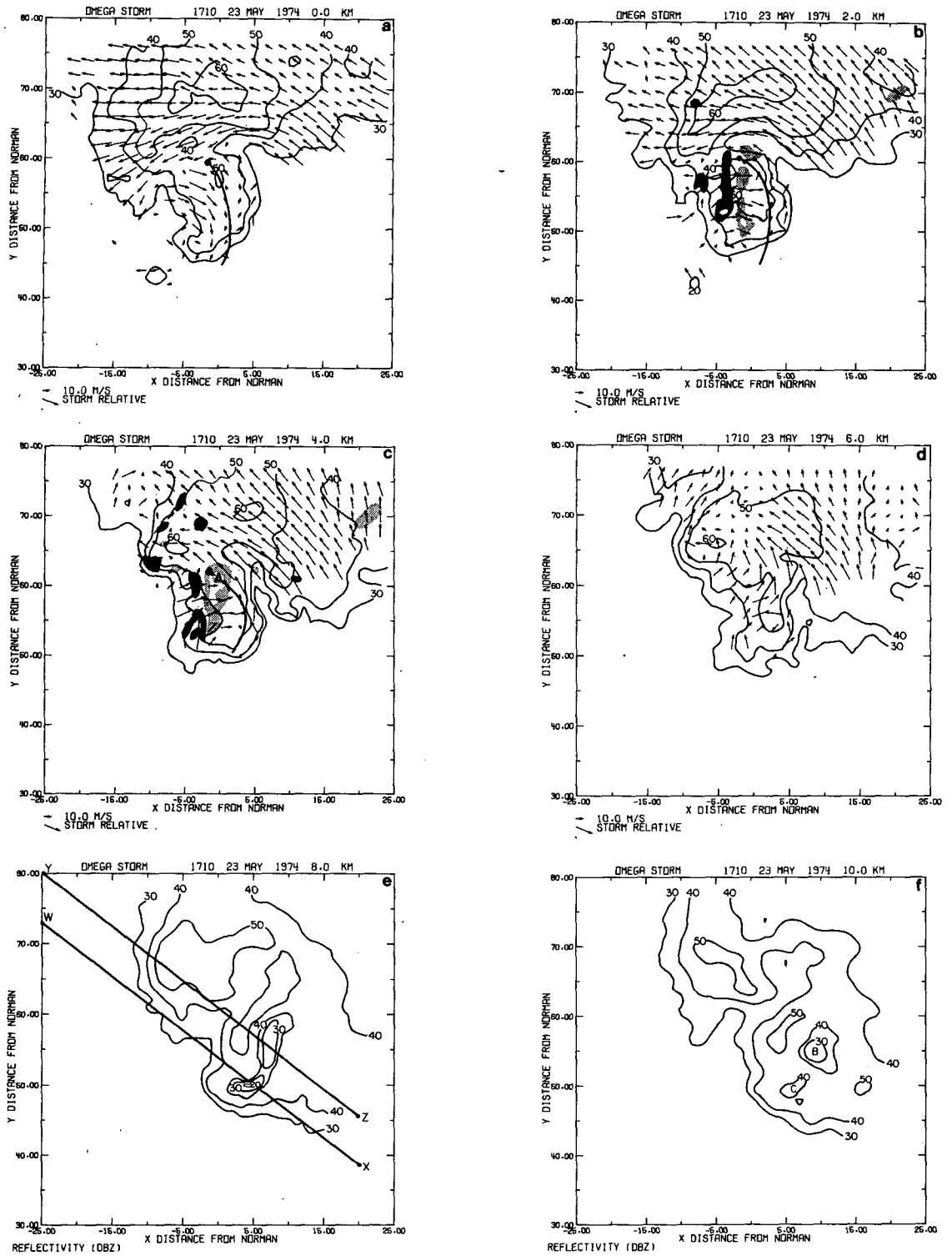

FIG. 5. Horizontal sections of reflectivity and wind fields relative to storm motion of the Omega storm at 1710 CST. Norman Doppler reflectivity values are the solid lines labeled at 10 dB(Z) intervals. Horizontal wind relative to storm motion is shown by velocity vectors with vector length proportional to wind speed. An example of a 10 m s^{-1} magnitude vector is shown in the lower left hand corner (a vector length of 1 km is equal to 10 m s^{-1}) along with the storm motion vector (305°/15 m s^{-1}). Updrafts are given by the light shaded regions at 10 m s^{-1} intervals. That is, the first shaded contour is updraft $\geq$ 10 m s^{-1}, interior unshaded region $\geq$ 20 m s^{-1}, interior shaded region $\geq$ 30 m s^{-1}, etc. Downdrafts are similarly displayed except dark shading is used. The solid dark line extending southward from the circulation center on the 1 and 2 km sections indicates the gust front boundary. Updraft A, is marked on the 4 km section and updrafts B and C on the 10 km section, respectively. Vertical sections shown by lines WX and YZ are given in Fig. 7.

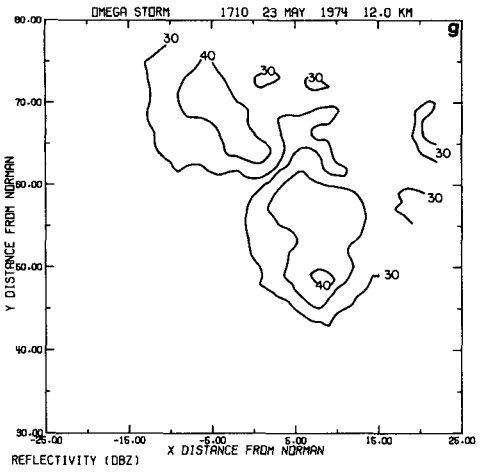

FIG. 5. (*Continued*)

from elongated southwest-to-northeast aligned echoes, forming large north–south aligned hook echoes as they moved from the northwest.

A dual-Doppler analysis at 1803 of the Yukon storm is shown in Fig. 8. Again, as in the case of the Omega storm, the hook echo is associated with a mesocyclone and there is evidence of multiple BWER's aloft (see 4 km section of Fig. 8). The BWER's are not as prominent as those on the Omega storm, but they may be somewhat obscured by the presence of radar reflective chaff. The chaff was released by aircraft at ~1755 at a height of 2.6 km in the position shown by the large dot on the 3 km section of Fig. 8 (Bensch, 1975). The chaff system was designed to release 2.5×10^6 dipoles through a vertical depth of ~2.5 km below the release altitude (McCarthy *et al.*, 1974). It is believed that the area immediately south of the west–east aligned horizontal bar shown on the 0 km section of Fig. 8 is reflective due to chaff and not precipitation particles. This is surmised because this area of the storm does not contain reflectors of this magnitude either before (radar data at 1756) or after (radar data at 1815) this time (see also Bensch, 1975). The vertical extent of the chaff is not known; however, in the 7.5 min between its launch and the map time of Fig. 8, it could have mixed to over 7 km in a 10 m s^{-1} updraft.

A striking dissimilarity to the Omega storm is that the Yukon storm's low level (<2.0 km) horizontal flow relative to the ground is from the northeast, whereas the Omega storm's low-level ground relative air motion (not shown) was southeasterly. The Yukon storm's northeasterly flow structure is evident not only in the storm's interior, but also ahead of the storm where velocities are obtainable from chaff signals. Surface equivalent potential temperature values and streamlines suggest that this northeasterly flow in the low-level environment resulted from Omega storm's outflow. These data indicate that much of the Yukon storm is imbedded in the outflow produced by the Omega storm. In fact, it appears that new updrafts form along the boundary of the Yukon's storm's gust front where it intersects the Omega outflow boundary. This is supported by the data shown in Fig. 9. Note the regular storm propagation between 1731 and 1751. Within 5 min after 1751, however, the pendant echo develops explosively southward and then forms another quasi-steady configuration that lasts past 1835. During this period, storm intercept personnel also reported towers growing explosively. The data indicate that the rapid southern reflectivity extension occurs in an area of enhanced

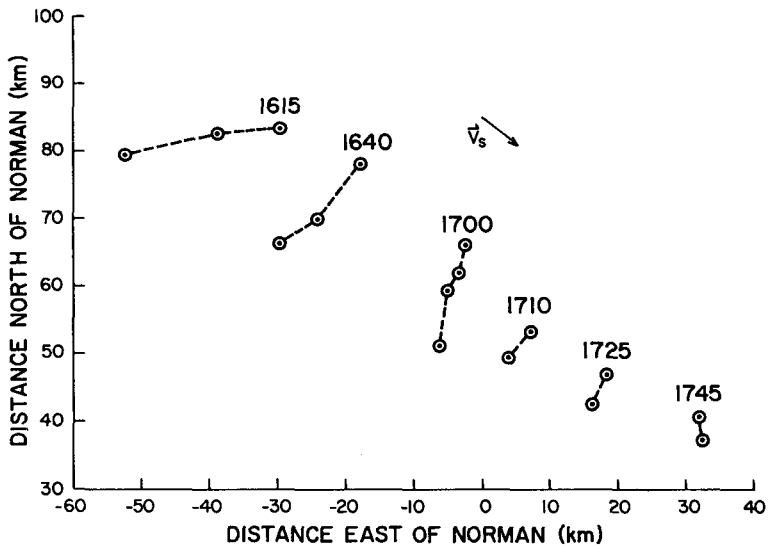

FIG. 6. Horizontal positions of Omega storm bounded weak echo regions (BWER's) at 6 km from 1615 to 1745 CST. Contemporary BWER's are joined by the dashed lines. Storm motion vector (305°/15 m s^{-1}) is also indicated.

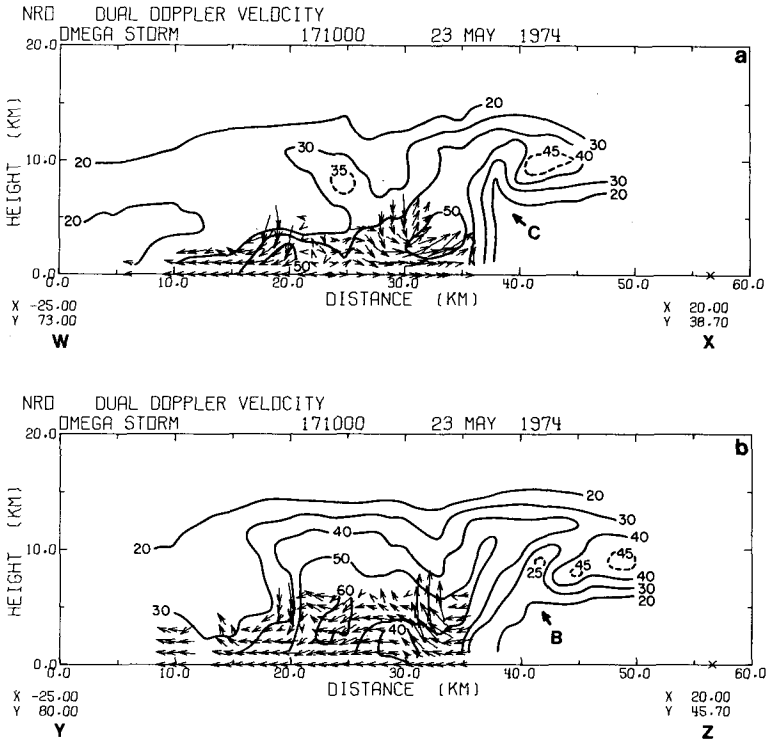

FIG. 7. Northwest-southeast oriented vertical sections through two BWER's of Omega storm. Norman Doppler reflectivity [dB(Z)] is shown by solid and dashed lines. Velocity vectors 1 km in length are equivalent to 10 m s^{-1} in speed (See Fig. 5 for further orientation).

convergence at the junction of the outflow boundaries from the two storms. The interaction between the two storms is better seen in composite drawings at 1745, 1803 and 1815 (Fig. 10). The heavy dashed line on the 1745 composite indicates the Omega storm's outflow boundary position based on information from surface stations, storm intercept teams and observations by a meteorologist at the Cimarron Doppler radar site. The position at this time is known quite accurately. Storm intercept photos from two separate locations allowed post-facto triangulation of cloud lines associated with both the Omega and, at a later time, the Yukon boundaries. Furthermore, a third intercept group crossed beneath the boundary separating Omega outflow from environmental air (at 1750) within 2 km of the Yukon storm. At 1745 the Omega outflow boundary stretches at least as far west as the El Reno (ELR) surface site. By 1803 this surface site has come under the influence of the Yukon storm's strong outflow and substantial new growth has caused the storm's pendant echo to extend southward. Due to lack of additional quantitative information, the Omega outflow boundary position at 1745 is only repeated on the 1803 and 1815 composites and not readjusted. Southeast winds at the Cimarron radar site, however, were observed to increase in magnitude as the storm approached, indicating, in a storm relative sense, that this boundary had not progressed far ahead of the storm. Also shown in the 1815 portion of Fig. 10 is the tornado damage track as determined from a ground survey. It is clear from this composite that the tornado did not come from the center of the main circulation, but instead is associated with new growth in the pendant echo near the junction of the outflow boundaries. The tornado formation mechanism is not known with certainty. It is interesting to note, however, that the Omega and Yukon storms both experienced the same environmental conditions and exhibited very similar life histories. The only major difference discerned by these investigators is the gust front interaction. Additionally, since the tornado formed at the junction of these boundaries, this suggests a causal relationship between the gust front intersection and the tornado.

4. Discussion

a. Gust fronts

Data from the severe thunderstorm cases of 23 May 1974 demonstrate that gust fronts played an important role in many aspects of the storms' life histories. As revealed by an animated sequence of satellite photographs, thunderstorms in Oklahoma were initiated at the intersection of a stationary cold

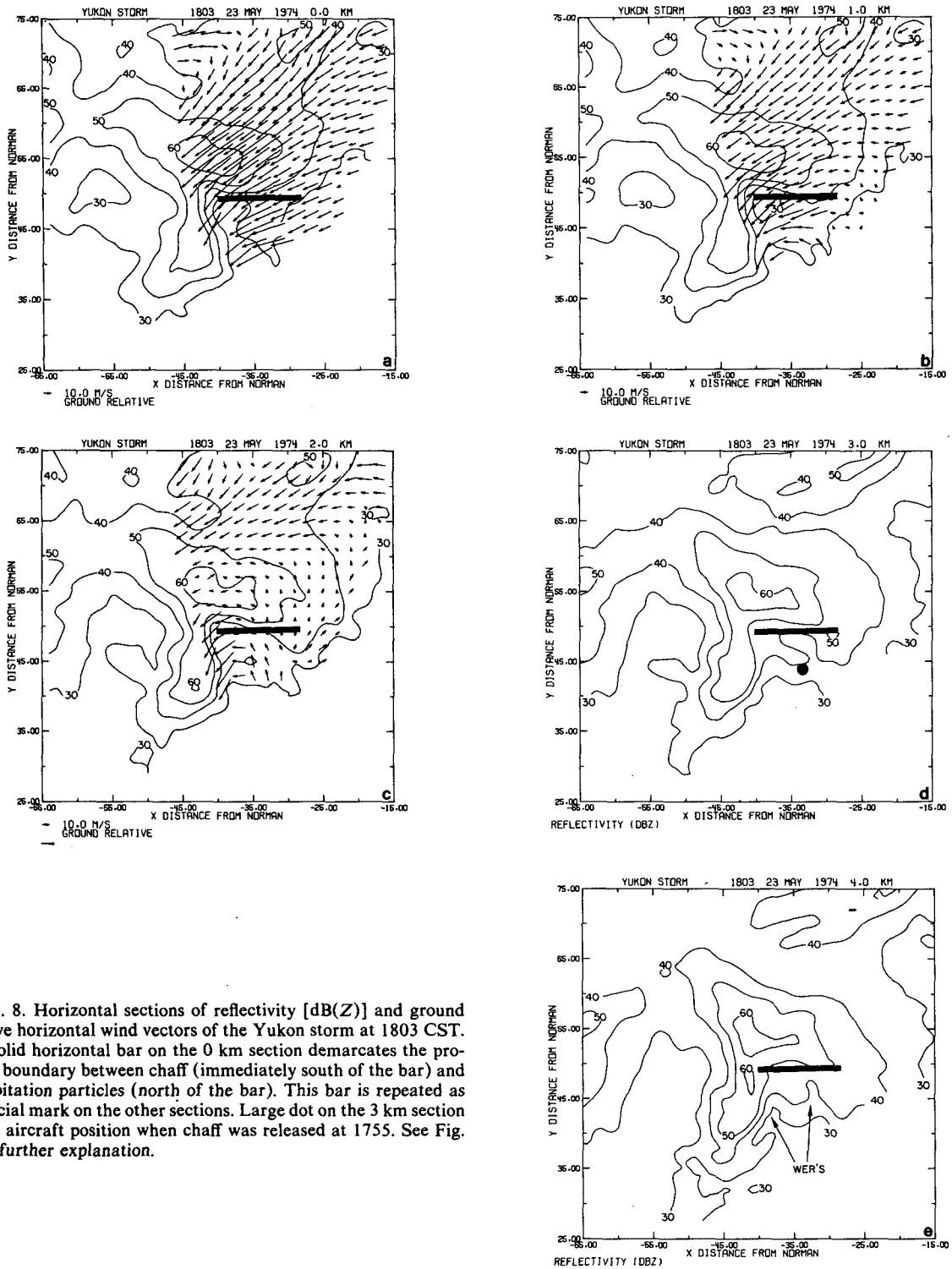

FIG. 8. Horizontal sections of reflectivity [dB(Z)] and ground relative horizontal wind vectors of the Yukon storm at 1803 CST. The solid horizontal bar on the 0 km section demarcates the proposed boundary between chaff (immediately south of the bar) and precipitation particles (north of the bar). This bar is repeated as a fiducial mark on the other sections. Large dot on the 3 km section shows aircraft position when chaff was released at 1755. See Fig. 5 for further explanation.

front with an outflow boundary from activity in Kansas. Further, propagation seemed to be governed by each storm's own gust front. Cells generally moved from west to east with the environmental winds, but system motion was toward the southeast due to discrete cell formation along the outflow boundary.

The data also revealed evidence of explosive growth in the Yukon storm as its gust front interacted with that of the Omega storm. This growth preceded by ~25 min the formation of a short-lived and weak tornado. It is interesting to note that this was the only tornado reported even though both

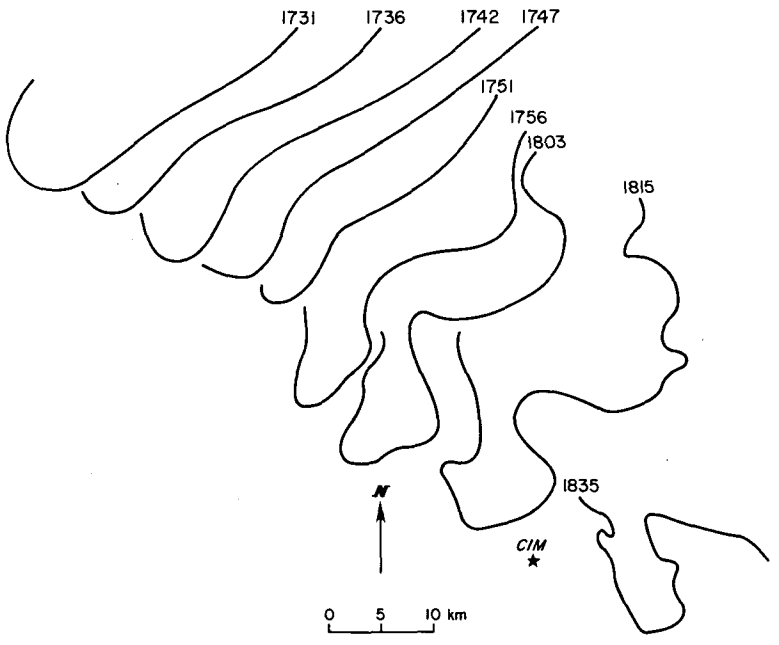

FIG. 9. Outline of Yukon storm's 0° elevation 45 dB(Z) echo from 1731 to 1835 CST.

storms possessed strong mesocyclones. This tornado did not form in the center of the Yukon storm's mesocyclone (Brandes, 1978; Burgess and Donaldson, 1979), but instead near the intersection of the outflow boundaries of the two storms, strongly suggesting the tornado formed because of this gust front interaction. Possible reasons for tornadogenesis include 1) an increase in low-level vorticity with the arrival of backed, northeasterly winds, 2) stretching of vortex tubes due to the increase in low level convergence and subsequent updraft intensification, or 3) some other, unknown process.

b. Storm structure

The structures of the storms on 23 May 1974 are sufficiently unusual to be worthy of comment. The most striking feature is that despite the storms' supercell type features (hook echoes, large bounded WER's), they propagated via growth of discrete new cells on their gust front boundaries. This view is at odds with the concept of supercell storms propagating continuously, and there is a growing body of evidence, such as the present study, indicating that such exceptions are not uncommon (e.g., Nelson and Braham, 1975; Lemon, 1976; Lemon *et al.*, 1978). Therefore, it seems likely that a storm's propagation mode is not a clear distinguishing characteristic between "supercell" and "multicell" storms. Any difference must lie in some other physical characteristic.

Visually the storm exhibited features not usually encountered by the NSSL mobile observation teams. During both the intensification of the mesocyclone circulation and occurrence of the tornado, an extensive outflow cloud (shelf cloud) swept southeastward from the wall cloud of the Yukon storm, before curving back toward the distant west. Storm spotters generally associate extensive outflow clouds with weakening storms; however, in this case, the shelf cloud had formed well before tornado occurrence. Instead of racing out far ahead of the storm to cut off the inflow, it remained quasi-steady with respect to the storm and had actually been drawn back into the storm near the mesocirculation, i.e., the gust front cloud had "wrapped back" into the storm.

c. Summary

In the foregoing, we have presented evidence of the extreme importance of outflow boundaries to all aspects of a storm's life. With so much current effort in the meteorological community being directed toward improved nowcasting techniques, thunderstorm gust front interaction seems a timely topic—worthy of major research. Experienced nowcasters realize that once a few storms are triggered, a region will probably be subjected to a round of activity lasting most of the evening and, perhaps, throughout the night. Improved techniques for sensing outflow boundaries would probably allow better understanding of location, timing and intensity of thunderstorm events, and ultimately improved predictions and warnings.

Acknowledgments. The authors wish to thank those involved with dispersal of the radar reflective

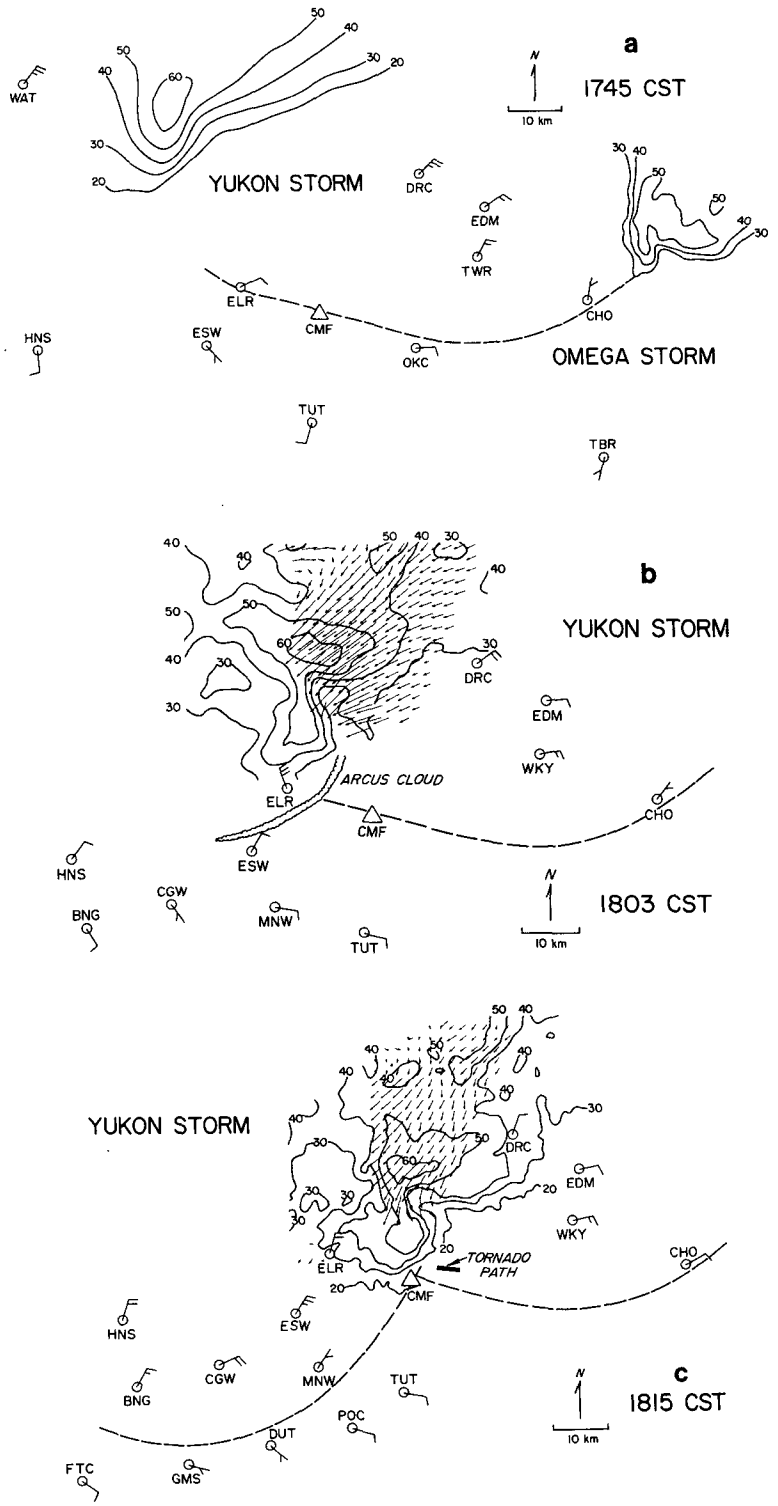

FIG. 10. Composite pictures of Doppler radar and surface data showing the relationship between the outflow boundaries of the Omega and Yukon storms. Reflectivity data [dB(Z)] in the 1745 section are from the NSSL WSR-57 radar (westernmost storm; Yukon storm) and the Norman Doppler (easternmost storm; Omega storm). The 1803 and 1815 reflectivity and ground relative wind vectors are the same format as described in Fig. 5. The Cimarron radar site (CMF) is shown by a triangle and surface sites by circles. A full wind barb is equivalent to 5 m s^{-1}. Storm outflow boundaries are indicated by the heavy dashed line. Note tornado damage path on the 1815 composite. The arcus cloud position at 1803 was determined from photographs and visual observations.

chaff: Mr. Randall Bensch and Drs. John McCarthy and Don Veal.

Mr. Vincent Wood developed the programs responsible for the three-dimensional perspective view shown in Fig. 4. Ms. Alice Adams assisted in some stages of the data analysis.

Visual observations, storm photographs and a tornado track by Mr. Don Burgess were invaluable to this study. We would also like to thank members of the National Severe Storms Laboratory and University of Oklahoma Tornado Intercept Projects for their important photographic and visual observations.

The figures were the products of much caring and work by Ms. Joan Kimpel, Mr. Bob Goldsmith and Mr. Charles Clark.

Ms. Sandy Mudd is sincerely thanked for her diligence and patience in typing various copies of the manuscript.

Partial support for the data collected in this study was from the Nuclear Regulatory Commission under Interagency Agreement AT(49-25)-1004.

REFERENCES

Alberty, R. A., J. F. Weaver, D. Sirmans, J. T. Dooley and W. C. Bumgarner, 1977: Spring Program 1976. NOAA Tech. Memo. ERL NSSL-83, 130 pp. [NTIS PB280745/AS].

Armijo, L., 1969: A theory for the determination of wind and precipitation velocities with Doppler radar. *J. Atmos. Sci.*, **26,** 570–573.

Barnes, S. L., 1973: Mesoscale objective map analysis using weighted time-series observations. NOAA Tech. Memo. ERL NSSL-62, 60 pp. [NTIS COM-73-10781].

——, 1978: Oklahoma thunderstorms on 29–30 April 1970. Part 1: Morphology of a tornadic storm. *Mon. Wea. Rev.*, **106,** 673–684.

Bensch, R. R., 1975: The circulation of a tornadic cyclone as revealed by single Doppler radar and chaff. *Preprints 9th Conf. Severe Local Storms*, Norman, Amer. Meteor. Soc., 91–95.

Bohne, A. R., and R. C. Srivastava, 1975: Random errors in wind and precipitation fall speed measurement by triple Doppler radar system. Lab. Atmos. Probing, Tech. Rep. No. 37, University of Chicago-Illinois Institute of Technology, 44 pp.

Brandes, E. A., 1978: Mesocyclone evolution and tornadogenesis: some observations. *Mon. Wea. Rev.*, **106,** 995–1011.

Brown, R. A., C. Safford, S. P. Nelson, D. W. Burgess, W. C. Bumgarner, M. L. Weible and L. Fortner, 1981: Multiple Doppler radar analysis of severe thunderstorms: Designing a general analysis system. NOAA Tech. Memo. ERL-NSSL-92, 21 pp.

Browning, K. A., and G. B. Foote, 1976: Airflow and hail growth in supercell storms and some implications for hail suppression. *Quart. J. Roy. Meteor. Soc.*, **102,** 499–533.

Burgess, D., and R. J. Donaldson, 1979: Contrasting tornadic storm types. *Preprints 11th Conf. Severe Local Storms,* Kansas City, Amer. Meteor. Soc., 84–89.

——, R. A. Brown, L. R. Lemon, and C. R. Safford, 1977: Evolution of a tornadic thunderstorm. *Preprints 10th Conf. Severe Local Storms*, Omaha, Amer. Meteor. Soc., 84–89.

Espy, J. P., 1841: *The Philosophy of Storms.* Charles C. Little & James Brown Co., 347 pp.

Fujita, T., 1958: Mesoanalysis of the Illinois tornadoes of 9 April 1953. *J. Meteor.*, **15,** 288–296.

——, 1960: Mesometeorological study of pressure and wind fields beneath isolated radar echoes. *Preprints 8th Weather Radar Conf.*, San Francisco, Amer. Meteor. Soc., 151–158.

——, and A. Pearson, 1976: Results of FPP classification of 1971 and 1972 tornadoes. *Proc. Symposium on Tornadoes,* Texas Tech University, Lubbock, 142–145.

Galway, J. G., 1956: The lifted index as a predictor of latent instability. *Bull. Amer. Meteor. Soc.*, **37,** 528–529.

Goff, R. C., 1976: Vertical structure of thunderstorm outflows. *Mon. Wea. Rev.*, **104,** 1429–1440.

Harrison, H. T., and W. Orendorff, 1941: Pre-cold frontal squall lines. Meteor. Circ. No. 16, United Air Lines, Training Center, Aurora, CO, 12 pp.

Holle, R. L., and M. Meier, 1980: Tornado formation from downdraft interaction in the FACE mesonetwork. *Mon. Wea. Rev.*, **108,** 1010–1028.

Humphreys, W. J., 1914: The thunderstorm and its phenomena. *Mon. Wea. Rev.*, **42,** 348–380.

Lemon, L. R., 1976: The flanking line, a severe thunderstorm intensification source. *J. Atmos. Sci.*, **33,** 686–694.

——, and C. A. Doswell III, 1979: Severe thunderstorm evolution and mesocyclone structure as related to tornadogenesis. *Mon. Wea. Rev.*, **17,** 1184–1197.

——, D. W. Burgess and R. A. Brown, 1978: Tornadic storm airflow and morphology derived from single-Doppler radar measurements. *Mon. Wea. Rev.*, **106,** 48–61.

Marwitz, J. D., 1972: The structure and motion of severe hailstorms. Part I. Supercell storms. *J. Appl. Meteor.*, **11,** 166–179.

McCarthy, J., G. M. Heymsfield and S. P. Nelson, 1974: Experiment to deduce tornado cyclone inflow characteristics using chaff and NSSL dual Doppler radars. *Bull. Amer. Meteor. Soc.*, **55,** 1130–1131.

McFarland, B., 1901: The thunderstorm: a new explanation of one of its phenomena. *Mon. Wea. Rev.*, **29,** 297–298.

Nelson, S. P., 1977: Rear flank downdraft: a hailstorm intensification mechanism. *Preprints 10th Conf. Severe Local Storms,* Omaha, Amer. Meteor. Soc., 521–525.

——, 1980: A study of hail production in a supercell storm using a Doppler derived wind field and a numerical hail growth model. NOAA Tech. Memo. ERL NSSL-89, 90 pp.

——, and R. R. Braham, 1975: Detailed observational study of a weak echo region. *Pure Appl. Geophys.*, **113,** 735–746.

Purdom, J. F. W., 1973: Meso-highs and satellite imagery. *Mon. Wea Rev.*, **101,** 180–181.

——, 1976: Some uses of high-resolution GOES imagery in the mesoscale forecasting of convection and its behavior. *Mon. Wea. Rev.*, **104,** 1474–1483.

——, and K. Marcus, 1982: Thunderstorm trigger mechanisms over the southeast United States. *Preprints 12th Conf. Severe Local Storms*, San Antonio, Amer. Meteor. Soc., 487–488.

Ray, P. S., C. L. Ziegler, W. Bumgarner and R. J. Serafin, 1980: Single and multi-Doppler radar observations of tornadic storms. *Mon. Wea. Rev.*, **108,** 1589–1606.

Staff, 1971: The NSSL surface network and observations of hazardous wind gusts. NOAA Tech. Memo. ERL NSSL-55, 20 pp. [NTIS COM-71-00910].

Suckstorff, G. A., 1939: Die Ergebnisse der Untersuchungen an tropischen Gewittern und einigen ander en tropischen Wetterscheinungen. *Gerlands Beitr. Geophys.*, **55,** 138–185.

Tepper, M., 1950: A proposed mechanism of squall lines: The pressure jump line. *J. Meteor.*, **7,** 21–29.

Weaver, J. F., 1979: Storm motion related to boundary-layer convergence. *Mon. Wea. Rev.*, **107,** 612–619.

Wilk, K. E., and E. Kessler, 1970: Quantitative radar measurements of precipitation. *Meteorological Observations and Instrumentation, Meteor. Monogr.*, No. 33, Amer. Meteor. Soc., 315–329.